

## Mortality following peripheral infection with Tick-borne encephalitis virus results from a combination of central nervous system pathology, systemic inflammatory and stress responses

Daisuke Hayasaka <sup>a,\*</sup>, Noriyo Nagata <sup>b</sup>, Yoshiaki Fujii <sup>c</sup>, Hideki Hasegawa <sup>b</sup>, Tetsutaro Sata <sup>b</sup>, Ryuji Suzuki <sup>c</sup>, Ernest A. Gould <sup>d,e</sup>, Ikuo Takashima <sup>f</sup>, Satoshi Koike <sup>a</sup>

<sup>a</sup> Department of Microbiology and Immunology, Tokyo Metropolitan Institute for Neuroscience, Tokyo Metropolitan Organization for Medical Research, 2-6 Musashidai, Fuchu, Tokyo 183-8526, Japan

<sup>b</sup> Department of Pathology, National Institute of Infectious Diseases, Gakuen 4-7-1, Musashimurayama, Tokyo 208-0011, Japan

<sup>c</sup> Clinical Research Center, National Hospital Organization Sagami Hospital, Sakuradai 18-1, Sagami, Kanagawa 228-8522, Japan

<sup>d</sup> Center for Ecology and Hydrology, Mansfield Road, Oxford OX2 8NN, UK

<sup>e</sup> Unité des Virus Emergents, Faculté de Médecine Timone, Marseille, France

<sup>f</sup> Laboratory of Public Health, Department of Environmental Veterinary Sciences, Graduate School of Veterinary Medicine, Hokkaido University, Sapporo 060-0818, Japan

### ARTICLE INFO

#### Article history:

Received 22 March 2009

Returned to author for revision 10 April 2009

Accepted 29 April 2009

Available online 24 May 2009

#### Keywords:

Tick-borne encephalitis virus

Mouse model

Mortality

Peripheral infection

Central nervous system pathology

Systemic inflammation

Systemic stress response

### ABSTRACT

Tick-borne encephalitis virus (TBEV) induces acute central nervous system (CNS) disease in humans. In this study, we investigate the pathogenetic mechanisms that correlate with fatal infection with TBEV in a mouse model. Following subcutaneous infection with high challenge doses ( $>10^7$  PFU), mice started to die early (8 days) and mortality rates reached  $>80\%$ . These doses induced acute and widespread infection of the CNS. On the other hand, following subcutaneous infection with low challenge doses ( $10^2$ – $10^6$  PFU), mice started to die late (11 days) and approximately one half of the mice survived but exhibited degrees of encephalitis similar to dying mice. However, low dose dying mice exhibited severe systemic stress response, and increased levels of TNF- $\alpha$  compared with recovering mice. We therefore conclude that in addition to the development of CNS disease, systemic inflammatory and stress responses contribute to induce a fatal infection following subcutaneous infection of mice with TBEV.

© 2009 Elsevier Inc. All rights reserved.

### Introduction

Tick-borne encephalitis virus (TBEV), which belongs to the genus *Flavivirus* in the family *Flaviviridae*, is a causative agent of acute central nervous system (CNS) disease in humans (Dumpis, Crook, and Oksi, 1999; Lindquist and Vapalahti, 2008). TBEV is prevalent over a wide area of Europe and Asia, and is geographically and genetically divided into three subtypes comprising the European, Siberian and far-eastern subtypes (Ecker et al., 1999; Hayasaka et al., 2001b). TBEV infects humans through the bite of an infected tick and the endemic areas of Europe and

Asia correspond to the geographical distribution of *Ixodes* tick species (Burke and Monath, 2001; Dumpis, Crook, and Oksi, 1999).

In human cases, Tick-borne encephalitis (TBE) characteristically takes a biphasic course involving an acute febrile illness, a period of apparent recovery, followed by a neurological syndrome (Holzmann, 2003; Lindquist and Vapalahti, 2008). The neurological symptoms include headache, meningitis, meningoencephalitis and meningoencephalomyelitis, the latter being observed in the most severe cases. When death follows, it is usually within 5 to 7 days of the onset of neurological signs (Dumpis, Crook, and Oksi, 1999). Such clinical features are not unique to TBE, thus, laboratory diagnosis is required to distinguish it from other neurological disorders (Charrel et al., 2004; Holzmann, 2003).

The pathological findings in the brains of human cases are nonspecific and lesions are located in the brain stem, cerebrum, cerebellar cortex, pons, cerebellum, thalamus and motor neurons (Dumpis, Crook, and Oksi, 1999; Gelpi et al., 2005; Gelpi et al., 2006). TBEV antigens are immunohistochemically detectable in lesions of the large neurons (Gelpi et al., 2005), suggesting that TBEV can infect neurons widespread throughout the brain. Hence, TBE may present

\* Corresponding author. Fax: +81 42 321 8678.

E-mail addresses: [hayasaka-ds@igakuken.or.jp](mailto:hayasaka-ds@igakuken.or.jp), [hayasaka@nagasaki-u.ac.jp](mailto:hayasaka@nagasaki-u.ac.jp) (D. Hayasaka), [nnagata@nih.go.jp](mailto:nnagata@nih.go.jp) (N. Nagata), [fyoshiki@nih.go.jp](mailto:fyoshiki@nih.go.jp) (Y. Fujii), [hasegawa@nih.go.jp](mailto:hasegawa@nih.go.jp) (H. Hasegawa), [tsata@nih.go.jp](mailto:tsata@nih.go.jp) (T. Sata), [r-suzuki@sagamihara-hosp.gr.jp](mailto:r-suzuki@sagamihara-hosp.gr.jp) (R. Suzuki), [eag@ceh.ac.uk](mailto:eag@ceh.ac.uk) (E.A. Gould), [takasima@igakuken.or.jp](mailto:takasima@igakuken.or.jp) (I. Takashima), [koike-st@igakuken.or.jp](mailto:koike-st@igakuken.or.jp) (S. Koike).

<sup>1</sup> Present address: Department of Virology, Institute of Tropical Medicine, Nagasaki University, 1-12-4 Sakamoto, Nagasaki, 852-8523. Fax: +8195 819 7830.

nonspecific clinical features associated with neurological symptoms due to the different sites at which neuronal dysfunctions occur in the CNS.

The laboratory mouse model is the most commonly employed system with which to study the CNS pathology of TBEV *in vivo* because mice develop neurological symptoms similar to those observed in humans and develop relatively comparable neurological dysfunction (Chiba et al., 1999; Pogodina and Savinov, 1964; Sokol, Libikova, and Zemla, 1959; Vince and Grcevic, 1969). Thus, death has been used as an index of pathogenesis and lethal dose has often been determined. Mouse infection, following either the subcutaneous or intradermal route, is considered to be a reproducible model of natural human infections that may result from the bite of an infected tick.

The pathogenetic process following experimental infection with TBEV is fundamentally similar to that of other encephalitic flaviviruses including Japanese encephalitis virus (JEV), West Nile virus (WNV) and Murray Valley encephalitis virus (MVEV) (Albrecht, 1968; Burke and Monath, 2001; Garcia-Tapia et al., 2007). From studies of encephalitic infections by these viruses, it is believed that initial virus replication occurs in dendritic cells (DCs) such as Langerhans cells at the site of infection, and the infected DCs migrate to draining lymph nodes. After viremia and replication in peripheral organs, virus invades the CNS and these hosts develop CNS disease, although the mechanism by which the blood-brain-barrier is crossed is not completely understood (Byrne et al., 2001; Dumpis, Crook, and Oksi, 1999; Robertson et al., 2009; Samuel and Diamond, 2006).

The CNS pathology of TBEV involves two distinct features, neuroinvasiveness and neurovirulence (Mandl, 2005; Monath, 1986). Direct intracerebral infection usually results in high mortality rates and 50% lethal doses ( $LD_{50}$ ) are often below 1 PFU (Chiba et al., 1999; Monath et al., 1980). Therefore, it is generally believed that after viruses enter the CNS, the host develops lethal encephalitis. Thus, mortality rates following direct intracerebral infection represent neurovirulence, whereas mortality following peripheral infection represents neuroinvasiveness (Mandl, 2005).

Interestingly, it is known that mice do not exhibit a normal dose response curve of mortality following peripheral infection with some strains of encephalitic flavivirus. This phenomenon was first reported in the 1940s (Lennette, 1944). Although the reason for these apparent discrepancies is not fully understood, it is generally considered that dose independence is attributable to the outcome of viral infections in peripheral tissues before CNS entry. However, this hypothesis is controversial, because some mice recovered from illness with neuropathological sequelae following peripheral infection (Chiba et al., 1999; Hayasaka et al., 2004; Hayasaka et al., 2001b; Hayasaka et al., 1999). Thus, it is considered likely that virus neuroinvasion following peripheral infection does not simply determine whether or not the mice will die; rather, mortality is determined after the development of CNS disease. Therefore, in order to understand the basis of dose independent mortality, it is necessary to examine the development of CNS pathology that relates to disease severity and mortality.

CNS pathology is the consequence of viral infection of the corresponding cells and the resulting inflammatory responses in the CNS. Direct viral infection of neurons is considered to be the major cause of neurological disease, because viral infections cause apoptosis or degeneration of neurons *in vivo* and *in vitro* (Couderc et al., 2002; Liao et al., 1997; Prikhod'ko et al., 2001; Shrestha, Gottlieb, and Diamond, 2003). In addition, recent studies have demonstrated that inflammatory responses in the CNS have immunopathological effects (Iwasaki et al., 1986; King et al., 2007). For the mechanism of CNS pathology following TBEV infection, Vince and Grcevic (1969) showed that peritoneal infections of mice with TBEV, exhibit distinct patterns of CNS pathology involving meningovascular, angioencephalotoxic and degenerative patterns. However, it is not known how, or if, these pathological features correlate with disease development and mortality.

Our previous studies in mice reported that the far-eastern subtype of TBEV Oshima strain, which was isolated in Japan (Takashima et al., 1997), has a pathogenetic potential common among TBE viruses (Chiba et al., 1999; Hayasaka et al., 2001b; Hayasaka et al., 1999). However, the detailed mechanisms of CNS pathology and mortality were not fully elucidated. Thus, the purpose of this study was to investigate these mechanisms by addressing the following questions (i) do morbidity and virus neuroinvasion directly correlate with mortality, (ii) do surviving mice develop the CNS pathology and (iii) does mortality result from a single or multiple mechanisms, following subcutaneous infection with TBEV?

## Results

### *Dose independent mortality in inbred mice after subcutaneous infection with the Oshima strain of TBEV*

Previous reports showed that the TBEV Oshima strain elicited dose independent mortality in outbred ICR mice following peritoneal infection (Chiba et al., 1999; Hayasaka et al., 2001a). Thus, we used inbred B6 mice in this study to eliminate the influence of the genetic background in outbred mice. Following subcutaneous infection of groups of mice with sequentially increasing doses, mice did not exhibit a normal dose dependent curve of mortality (Fig. 1A). Two distinct mortality rate responses were observed one in which more than 80% of the mice died following a high virus challenge dose ( $10^7$  or  $10^{7.8}$  PFU) and the other in which 40 to 60% of the mice died following a lower virus challenge dose (from  $10^2$  to  $10^6$  PFU) (Fig. 1A). It is important to emphasize that in this lower challenge dose category there was no obvious difference in mortality rates at any of the challenge doses, even though the doses differed by several orders of magnitude.

Following high dose infections, mice started to die at 8 days post infection (pi) (Fig. 1B) and mean survival times (MSTs) were  $12.8 \pm 3.1$  days without significant differences between  $10^7$  and  $10^{7.8}$  PFU as the challenge dose. On the other hand, following the lower challenge dose infections, mice did not start to die until 11 days pi (Fig. 1B) and MSTs were  $15.8 \pm 2.9$  days with no significant difference between the challenge doses ( $10^2$  to  $10^6$  PFU). However, there was a significant difference in MSTs between high and low challenge doses ( $P < 0.01$ ).

### *Morbidity in mice*

All TBEV-infected mice remained asymptomatic for several days following infection, and then exhibited generalized clinical signs involving weight loss, slowness in movement, ataxia, piloerection and anorexia. Elevated body temperature was not observed, but hypothermia was induced (data not shown). Some mice exhibited neurological signs of paralysis involving rigidity and flaccid paralysis from 7 to 11 days pi.

In particular, body weight loss was the first clinical observation. Thus, we estimated the onset of disease by whether or not the weight of each mouse decreased compared with control uninfected mice. As shown in the survival curves (Fig. 1B), high dose infections elicited early onset of weight loss, whereas low dose infections induced delayed onset (Fig. 1C). The mean times to the onset of weight loss were  $6.4 \pm 0.49$  and  $8.1 \pm 0.96$  days pi following high or low dose infections, respectively.

### *Virus neuroinvasion alone does not induce fatal infection*

It is important to note, that morbidity rates did not correlate directly with mortality rates since all low challenge doses ( $> 10^2$  PFU) induced morbidity in 100% of mice regardless of whether or not they survived infection (Fig. 1D). All brains infected with  $> 10^2$  PFU of TBEV

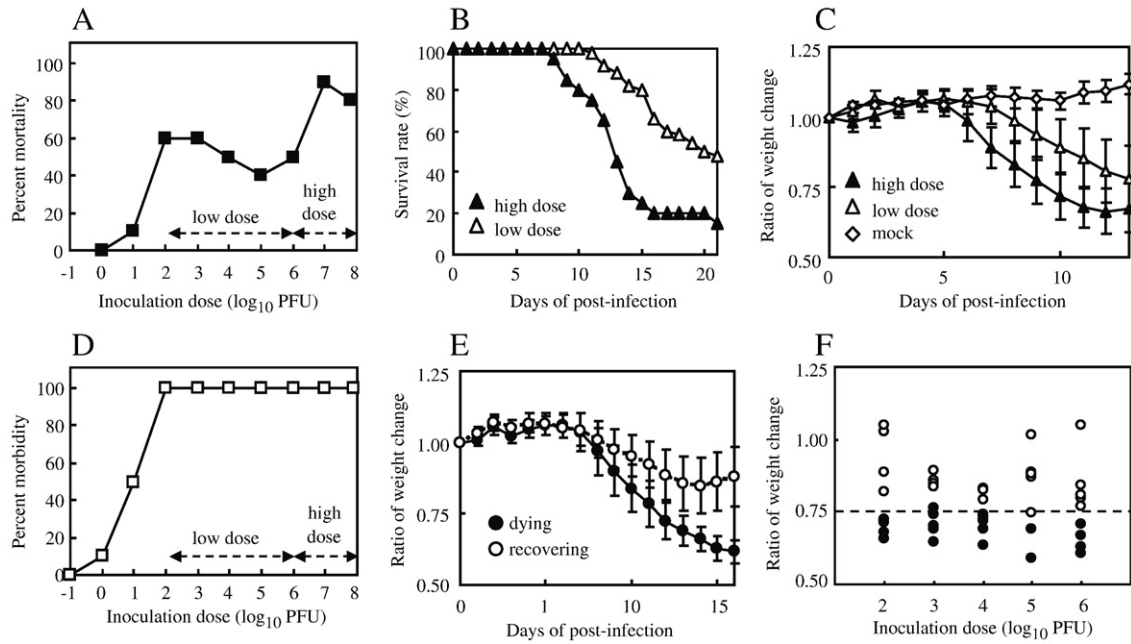


**Fig. 1.** Mortality and morbidity following subcutaneous infection with TBEV Oshima strain in B6 mice. Ten mice in each group were subcutaneously infected with increasing concentrations of virus ranging from 10<sup>-1</sup> to 10<sup>7.8</sup> PFU. Mortality rates (A) and survival curves (B) were recorded for 21 days after high (10<sup>7</sup> and 10<sup>7.8</sup> PFU) and low (10<sup>2</sup> to 10<sup>6</sup> PFU) dose infections and none of the mice died after 21 days. Mice were monitored daily for signs of disease and the average ratios of weight change of living mice at the time points compared with those of day 0 were recorded following high (10<sup>7</sup> and 10<sup>7.8</sup> PFU) and low (10<sup>2</sup> to 10<sup>6</sup> PFU) dose infection (C). Error bars represent the standard deviations. Morbidity of mice was estimated by degree of weight loss after 21 days (D). The averages of daily weight change of surviving or dying mice were monitored after low dose infections (E). Error bars represent the standard deviations. Individuals of surviving or dying mice were plotted in the degree of weight ratio at 13 days post infection (F).

contained infectious virus at 9 to 11 days pi when mice exhibited weight loss, but viral loads did not show a dose dependent correlation (data not shown).

Moreover, 20% of the surviving mice had presented with apparent neurological signs, including hind-limb hemiparesis following recovery, whereas 80% of the dead mice exhibited paralysis before death. Thus, since CNS disease was observed in both surviving and non-

surviving mice, neuroinvasiveness is not a sufficient condition to ensure a fatal consequence.

*Discrimination of dying and recovering mice*

Although surviving mice also exhibited virus neuroinvasion and clinical disease symptoms, it was uncertain if these mice actually

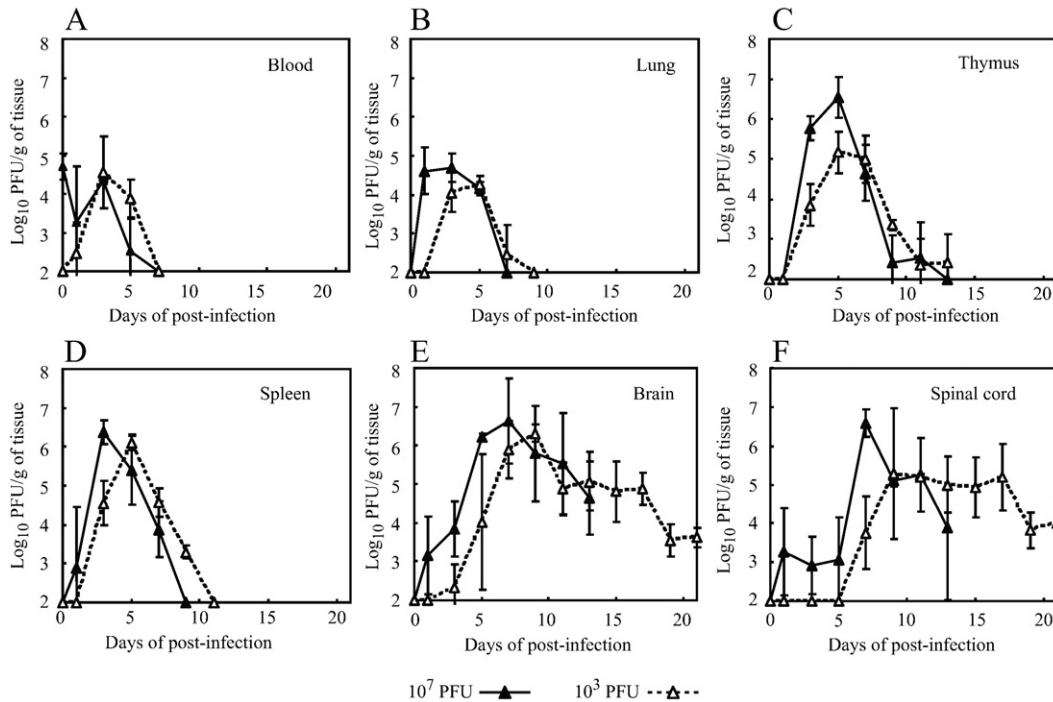


**Fig. 2.** Virus replication in peripheral organs and CNS following high (10<sup>7</sup> PFU) or low (10<sup>3</sup> PFU) dose infections. Titers per g of tissue represent the average from three to five mice in blood (A), lung (B), thymus (C), spleen (D), brain (E) and spinal cord (F). Error bars indicate the standard deviations.



developed CNS pathology. Thus, to confirm the CNS pathology and the correlation with mortality, we needed to be able to discriminate between dying and recovering mice during the observation period. To achieve this we followed the progression of weight change of mice that died or survived following low challenge doses. Mice that died exhibited continuous weight loss until death, whereas survivors

regained weight from 13 to 15 days pi (Fig. 1E), but the day of onset of weight loss was not significantly different. In fact, dead mice and survivors were clearly distinguished by whether or not mice showed less than 0.75 of the weight ratio, 13 days pi (Fig. 1F). From these observations, we could discriminate dying and recovering mice by the degree of weight change during the later period of infection.

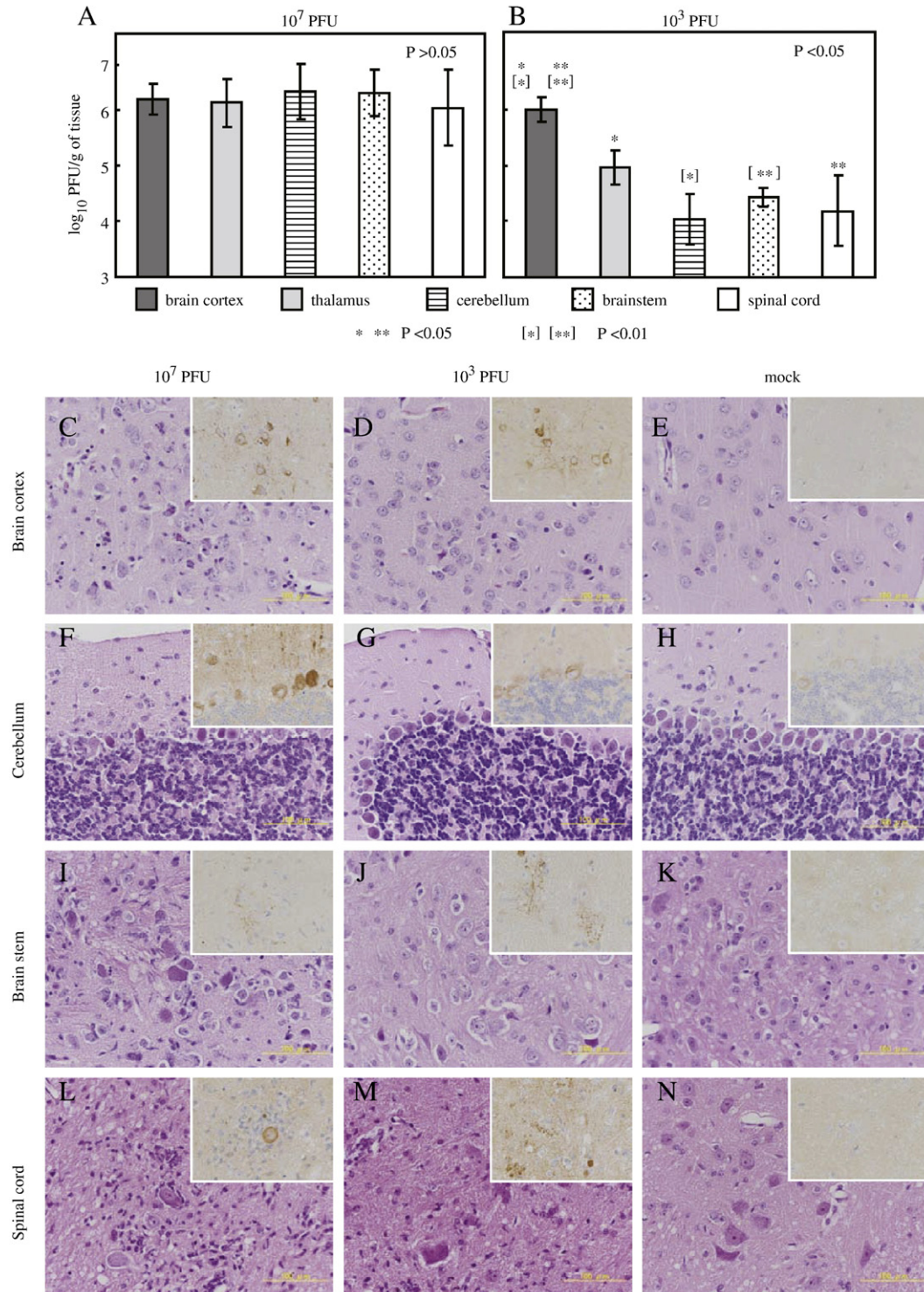


**Fig. 3.** Viral loads in distinct regions of the CNS and their histopathological features at early periods following infection. Viral loads in brain cortex, thalamus, cerebellum, brainstem and spinal cord of five mice infected with  $10^7$  PFU (A) or  $10^3$  PFU (B) infections at 7 days pi. The error bars indicate the standard errors. *P* value in each graph was determined by the analysis of variance. Asterisks show the pairs that exhibit significant differences by Student *T* test in the graph that indicates  $P < 0.05$  by the analysis of variance. Histopathology of brain cortex (C to E), cerebellum (F to H), brainstem (I to K) and spinal cord (L to N) in mice infected with  $10^7$  PFU (C, F, I and L),  $10^3$  PFU (D, G, J and M) and mock (E, H, K and N) at 8 days pi. TBEV antigens were detected using E protein specific TBEV antibody (insets). Each experiment represents three mice.

### Virus replication in mice

A major cause of disease development is considered to be direct viral infection and replication in the CNS. Therefore, we followed the development of viral load in mice following peripheral challenge with high ( $10^7$  PFU) or low ( $10^3$  PFU) infectious doses to look for evidence of a correlation between viral replication, disease development and time of death.

Following a high challenge dose infectious virus was detected from 0 to 3 days pi in blood, lung, thymus and spleen, and peaked 1 to 2 days later (Figs. 2A to D). On the other hand, following a low challenge dose, initial virus replication and/or the peak levels were delayed 1 to 2 days compared with the high challenge dose, although overall viral loads were not significantly different (Figs. 2A to D). Either of the challenge doses was reduced to below detection limits by approximately 10 days pi. Therefore, virus replication in peripheral organs did not appear to correlate with the progression of disease to death.

In CNS, following high challenge doses, infectious virus was detectable in the brain and spinal cord at 1 day pi, indicating that virus replication in CNS occurred almost simultaneously with replication in the peripheral organs (Figs. 2E and F). On the other hand, following the low challenge dose, infectious virus was detected on days 3 and 7 pi in brain and spinal cord, respectively (Figs. 2E and F). Thus,

these observations probably explain the different lengths of time of illness onset between high and low challenge doses (Fig. 1C).

The peaks of viral loads in CNS were 7 days pi following high dose infections (Figs. 2E and F), indicating that mice started to die at around the peak of viral load in the CNS. On the other hand, the peaks were 9 days pi following low dose infections (Figs. 2E and F). Subsequently, as the time post-infection increased, CNS viral loads gradually decreased (Figs. 2E and F), indicating that mice died during clearance of virus from the CNS. These data suggest that the mechanism of death is different in high and low challenge doses.

It is important to note that infectious virus was detected in the CNS of all mice infected with either high or low challenge doses even at 21 days pi by which time surviving mice had completely recovered from weight loss (Figs. 2E and F). Thus, virus neuroinvasion still occurs in all mice that survive infection.

### CNS pathology in mice at early days post infection

Since high but not low challenge dose caused early death (Fig. 1B), we compared CNS pathology early after infection with either high or low challenge doses. High challenge dose ( $10^7$  PFU) infections resulted in high viral loads with more than  $10^6$  PFU per g of tissue in every region of the CNS tested without significant differences (Fig. 3A). In contrast, a low challenge dose ( $10^3$  PFU) resulted in significantly lower

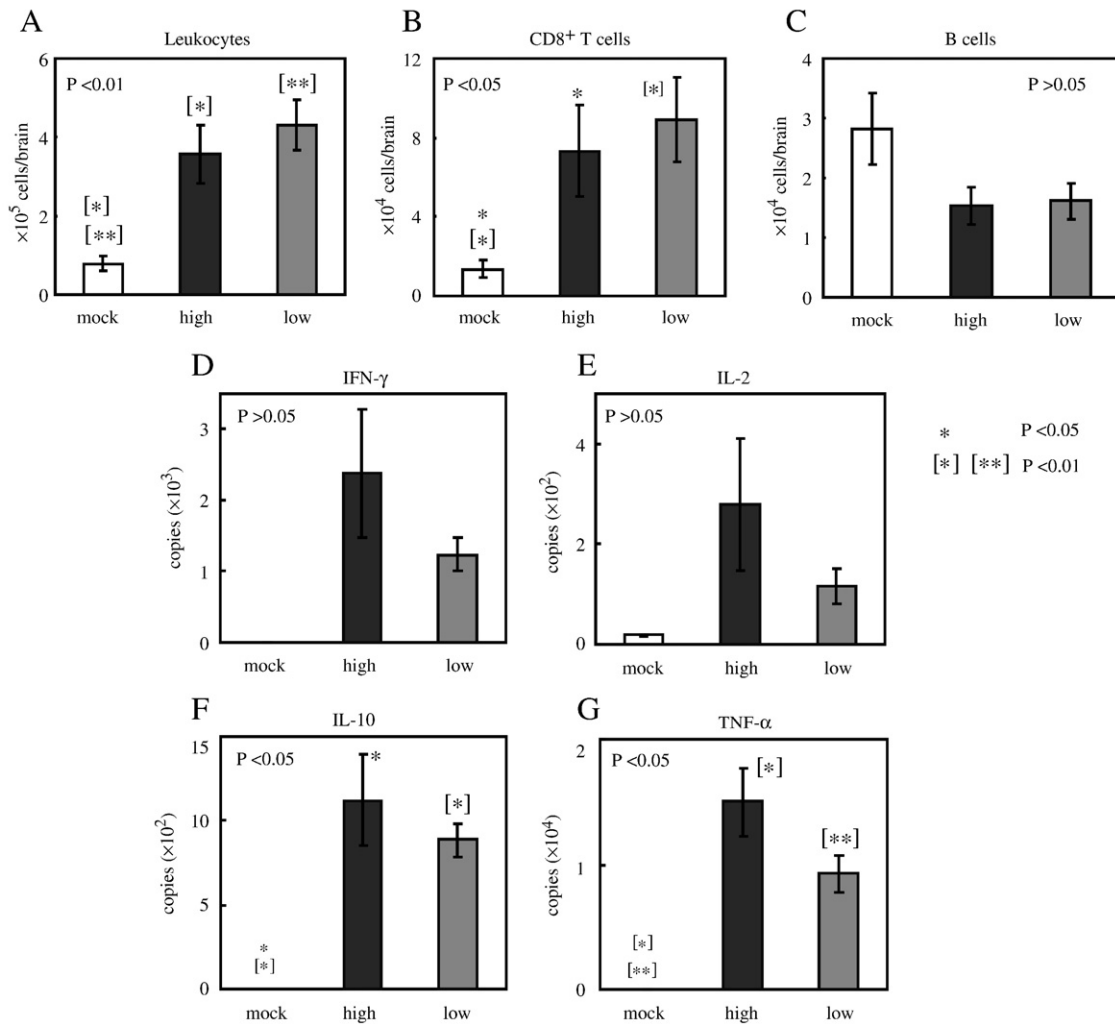


**Fig. 4.** Inflammatory responses in brains at 8 days pi after infection with mock,  $10^7$  PFU or  $10^3$  PFU per mouse. Number of infiltrating leukocytes (A), CD8<sup>+</sup> T cells (B) and B cells (C) in brains of five mice per group. Inflammatory cytokines in brains of five mice in each group at 8 days pi were quantified by real-time PCR. The expression levels of mRNA of IFN- $\gamma$  (D), IL-2 (E), IL-10 (F) and TNF- $\alpha$  (G) are shown as the copy numbers compared to  $10^7$  copies of GAPDH mRNA. Error bars indicate the standard errors. P value in each graph was determined by the analysis of variance. Asterisks show the pairs that exhibit significant differences by Student *T* test in the graph that indicates  $P < 0.05$  by the analysis of variance.



viral loads in the thalamus, cerebellum, brainstem and spinal cords compared with that of the brain cortex; in which viral load was similar to the high challenge dose (Fig. 3B).

Corresponding to the viral loads, histopathological examination showed that acute necrotic neurons with TBEV antigens and inflam-

matory reactions were observed widely throughout the CNS involving brain cortex (Fig. 3C), thalamus (data not shown), cerebellum (Fig. 3F), brainstem (Fig. 3I) and spinal cord (Fig. 3L) following the high challenge dose. On the other hand, following the low challenge dose, some necrotic neurons displayed TBEV antigens and slight

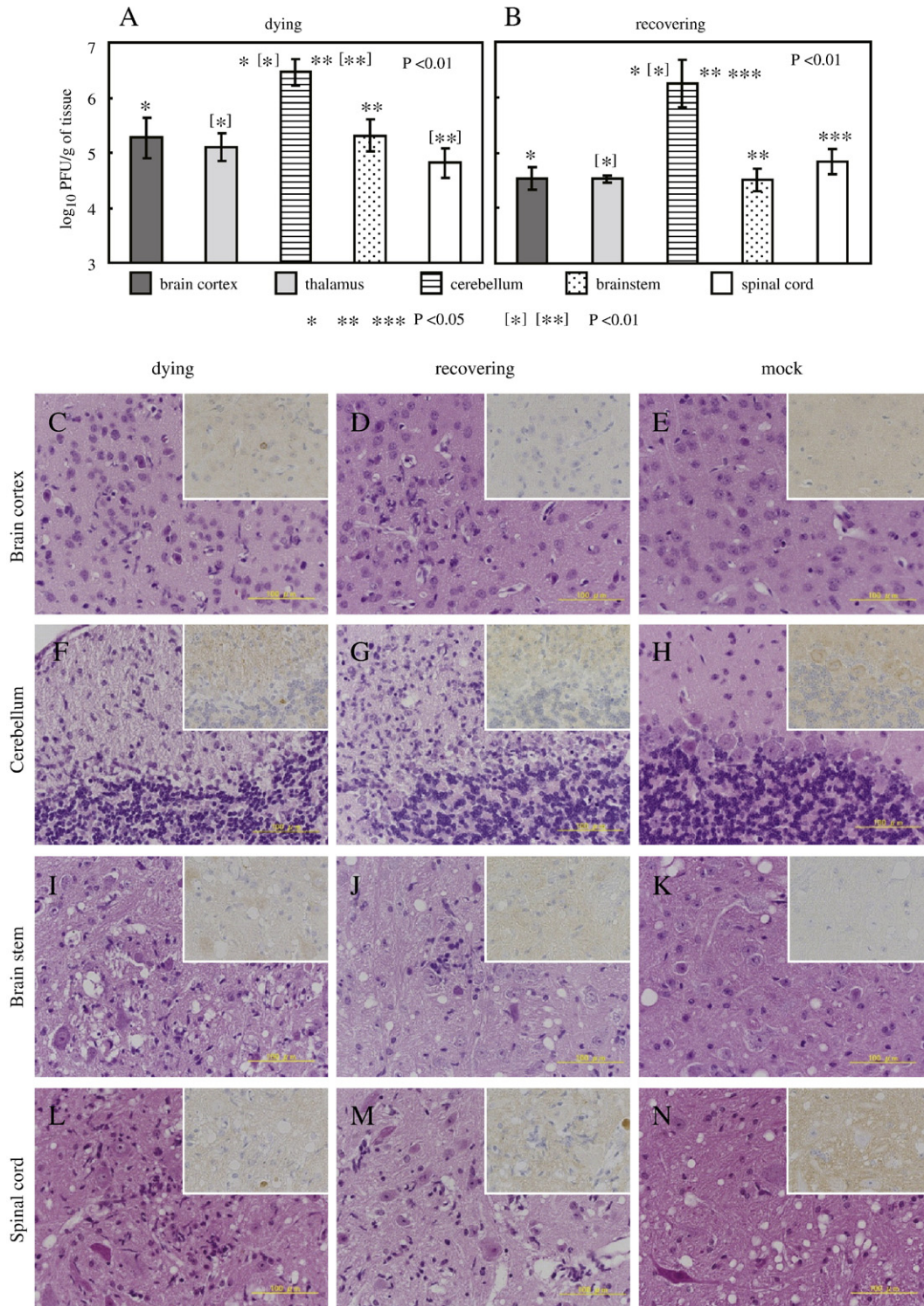


**Fig. 5.** Viral loads and the histopathological features in CNS during the late period of infection after 10<sup>3</sup> PFU dose. Dying and recovering mice were distinguished whether the degree of weight loss was more or less than 0.75. Viral loads in brain cortex, thalamus, cerebellum, brainstem and spinal cord of five mice either dying (A) or recovering (B), at 13 days pi. The error bars indicate the standard errors. P value in each graph was determined by the analysis of variance. Asterisks show the pairs that exhibit significant differences by Student T test in the graph that indicates P < 0.05 by the analysis of variance. Histopathology of brain cortex (C to E), cerebellum (F to H), brainstem (I to K), and spinal cord (L to N) in dying mice (C, F, I and L), and recovering mice (D, G, J and M) and mock-infected mice (E, H, K and N) at 15 days pi following challenge with 10<sup>3</sup> PFU per mouse. TBEV antigens were detected with TBEV-specific E protein antibody (insets). Each experiment represents three mice.

cuffing was also observed in the brain cortex (Fig. 3D), thalamus (data not shown), cerebellum (Fig. 3G), brainstem (Fig. 3J) and spinal cord (Fig. 3M), but the degree of neuronal degeneration was lower in cerebellum, brainstem and spinal cord when compared with that following high challenge doses (Figs. 3G, J and M). In particular, Purkinje cells were still intact following low dose infection (Fig. 3G), but they showed severe degeneration following high dose infection (Fig. 3F). Mock-infected mice showed no neuronal degeneration, TBEV antigens or inflammatory reactions (Figs. 3E, H, K and N).

The inflammatory responses were assessed by measuring cell infiltration and levels of inflammatory cytokines present in brains at 8 days pi. Infiltrating leukocyte levels were significantly increased in both high and low challenge dose groups of mice compared with mock-infections (Fig. 4A). CD8<sup>+</sup> T cells (Fig. 4B), CD4<sup>+</sup> T cells, neutrophils and natural killer cell levels (data not shown) were also significantly increased, whereas B cell (Fig. 4C) and macrophage levels (data not shown) were decreased. However, there was no correlation between these increases or decreases with virus challenge dose. Inflammatory cytokine levels of IFN- $\gamma$ , IL-2, IL-10 and TNF- $\alpha$  also increased but again there was no correlation with virus challenge dose (Figs. 4D to G). Whilst individual levels of cytokines tended to be higher in high virus challenge dose mice, the differences were not significant (Figs. 4D to G).

Thus, the results suggest that early death following high virus challenge dose, primarily results from acute neurological dysfunction throughout the CNS directly due to viral cytopathic effects rather than generalized immunopathological effects.

#### CNS pathology in mice at late days post infection following low challenge dose

We subsequently investigated the CNS pathology in low challenge dose mice ( $10^3$  PFU) as above. In mice dying at 13 days pi, the viral load in brains was  $10^{5.7 \pm 0.20}$  PFU per g of tissue. This titer was lower than the peak levels ( $10^{6.3 \pm 0.11}$  PFU per g of tissue), although the difference was not significant. In recovering mice at 13 days pi, the viral load in brains was  $10^{5.4 \pm 0.21}$  PFU per g of tissue without significant difference from that of dying mice. However, interestingly, the viral load in the cerebellum was significantly increased ( $10^{6.5 \pm 0.24}$  and  $10^{6.5 \pm 0.24}$  PFU per g of tissue) compared with that observed earlier, i.e. at 7 days pi ( $10^{4.0 \pm 0.44}$  PFU per g of tissue) in both dying and recovering mice (Figs. 5A and B). In other words, the viral load in the cerebellum was significantly higher than that in the brain cortex, thalamus, brainstem and spinal cord (Figs. 5A and B). These observations indicate that viral infection alone is not a critical determinant of late death, unlike that of early death.

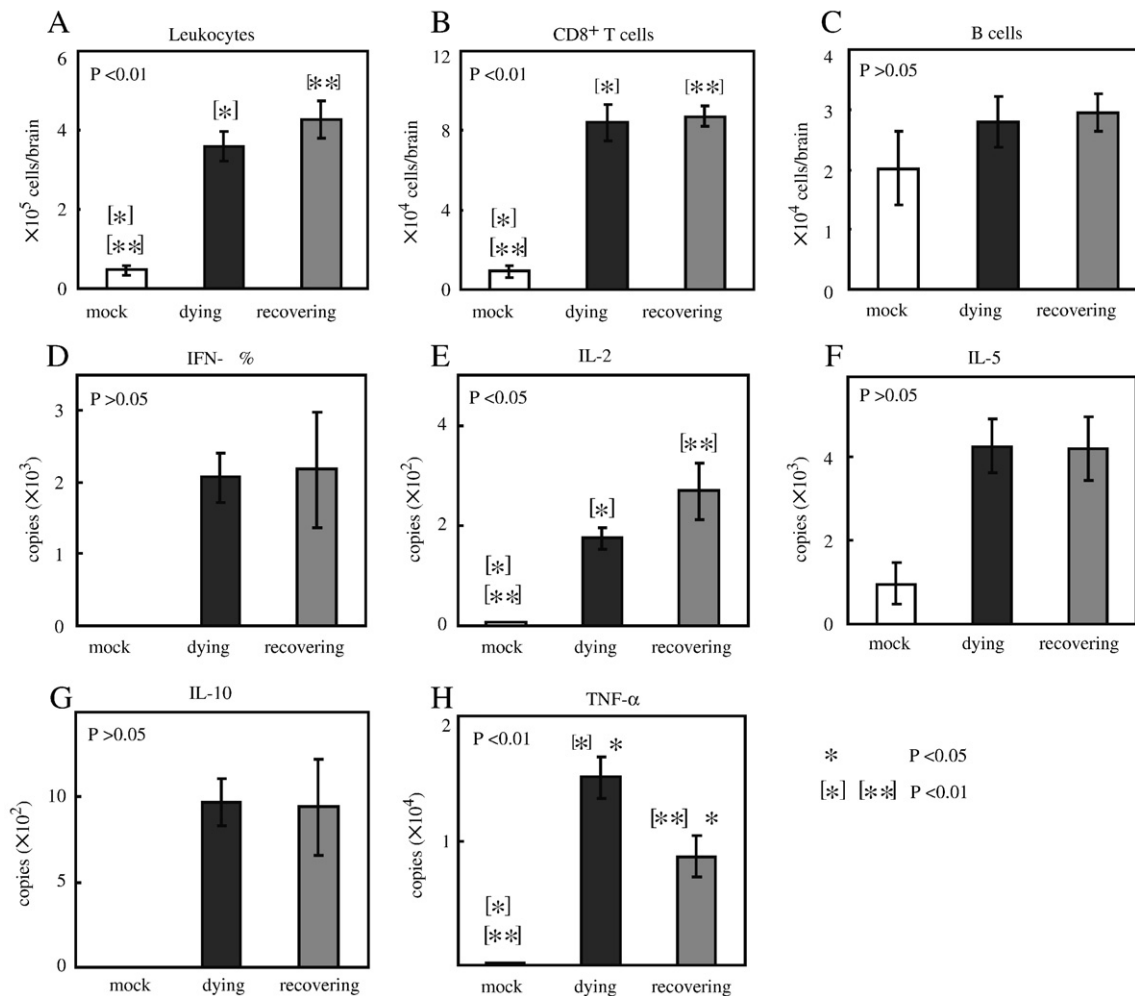


**Fig. 6.** Inflammatory response in brains of dying and recovering mice at late time of infection following either mock or  $10^3$  PFU challenge doses. Number of infiltrating leukocytes (A), CD8<sup>+</sup> T cells (B) and B cells (C) in brains of five mice per group at 13 days pi. Inflammatory cytokines in brains of five mice in each group at 13 days pi were quantified by real-time PCR. The expression levels of mRNA of IFN- $\gamma$  (D), IL-2 (E), IL-5 (F), IL-10 (G) and TNF- $\alpha$  (H) are shown as the copy numbers compared to  $10^7$  copies of GAPDH mRNA. Error bars indicate the standard errors. P value in each graph was determined by the analysis of variance. Asterisks show the pairs that exhibit significant differences by Student T test in the graph that indicates  $P < 0.05$  by the analysis of variance.

In both dying and surviving/recovering mice, histopathological examination showed inflammatory reactions with focal proliferation of microglial rod cells in the brain cortex (Figs. 5C and D), thalamus (data not shown), cerebellum (Figs. 5F and G), brainstem (Figs. 5I and J) and spinal cord (Figs. 5L and M). Severe inflammatory infiltration with mononuclear cells and rod shaped microglia were observed in the cerebellum, meninges and cortex with degenerate Purkinje cells (Figs. 5F and G). TBEV antigens were not detected or only weakly detected in cell debris (Figs. 5F and G). These pathological features were not observed in mock-infected mice (Figs. 5E, H, K and N).

The numbers of infiltrating leukocytes were increased in both dying and surviving/recovering mice compared with mock-infected mice (Fig. 6A). Levels of CD8<sup>+</sup> T cells (Fig. 6B), B cells (Fig. 6C), CD4<sup>+</sup> T cells, neutrophils, natural killer cells and macrophages (data not shown) were also increased. In both dying and surviving/recovering mice, the levels of inflammatory cytokines involving IFN- $\gamma$ , IL-2, IL-5, IL-10 and TNF- $\alpha$  in the brain were increased compared with mock-infected mice (Figs. 6D to G). Although the levels of TNF- $\alpha$  increased, they were lower in recovering mice than in dying mice (Fig. 6H).

Taken together, these observations suggest that following low challenge dose, mice developed encephalitis but showed features of

virus clearance from the CNS. Moreover, increased viral infections in the cerebellum with degenerating Purkinje cells were characteristically observed. However, for death to occur, whilst the development of CNS pathology is essential, it does not determine fatality following subcutaneous infection of mice with TBEV.

#### Systemic stress responses in dying mice

Since CNS pathology was detected in both surviving and dying mice, we have concluded that neurological dysfunction alone does not determine mortality. Therefore, we compared the peripheral pathology and systemic responses of dying and surviving mice.

Although the histopathological features in peripheral organs were not significantly different (data not shown), severe atrophy of the thymus and spleen were seen only in dying mice. Indeed, the numbers of thymocytes and splenocytes were dramatically decreased in dying mice compared with mock-infected mice and surviving mice (Figs. 7A and B). Significant reduction of CD4<sup>+</sup> and CD8<sup>+</sup> double positive cells were the main cause of thymus atrophy (Fig. 7C). On the other hand, overall phenotypes of splenocytes appear to be decreased (data not shown). Viral loads were below detection limits in both thymus and

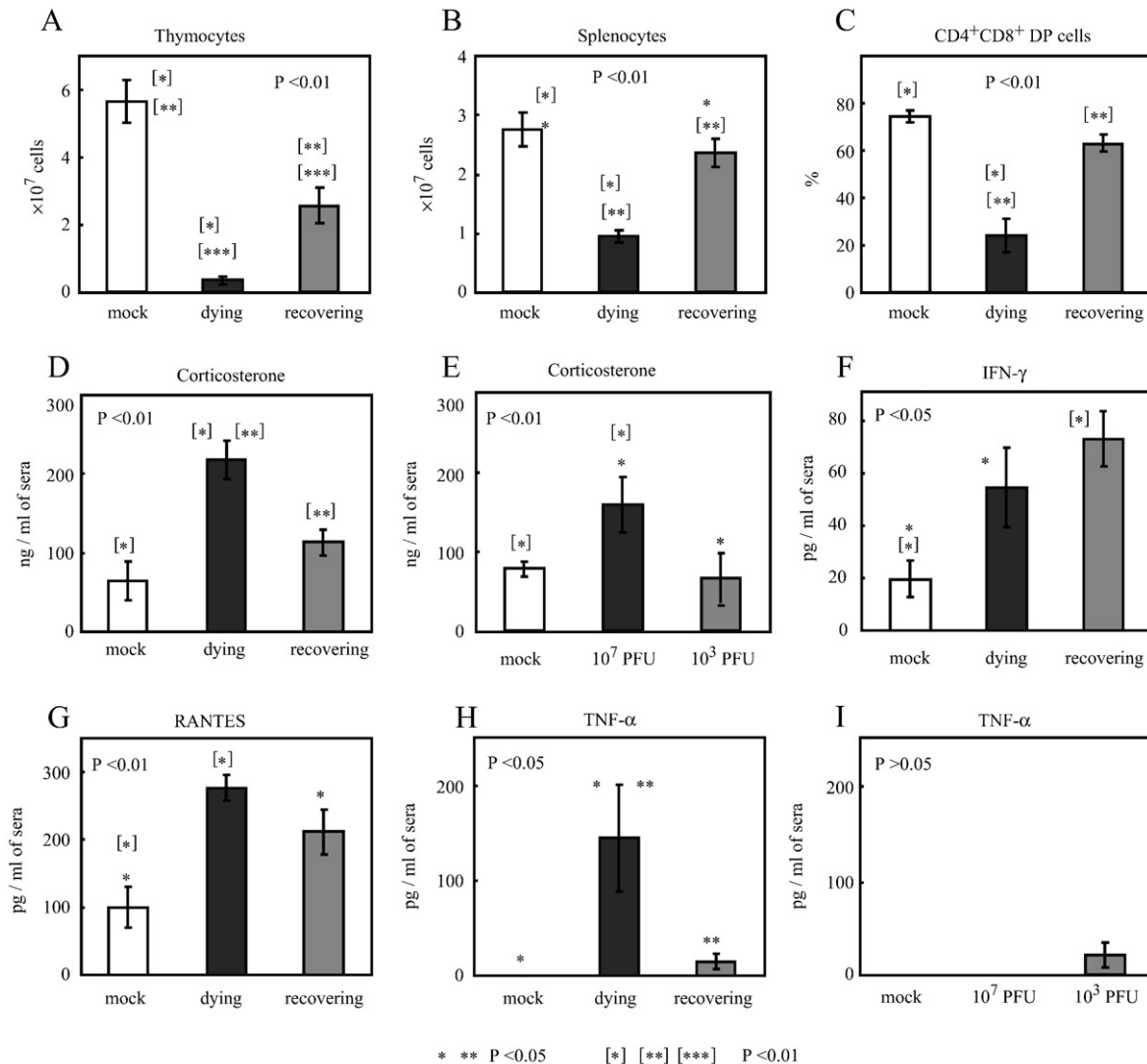


**Fig. 7.** Systemic stress response and expression of inflammatory cytokines in mice following a challenge dose of 10<sup>3</sup> PFU at 13 days pi. The number of thymocytes (A) and splenocytes (B), and the percentage expression CD4<sup>+</sup>CD8<sup>+</sup> double positive cells (C) in dying and recovering mice are represented. The level of corticosterone (D), IFN- $\gamma$  (F), RANTES (G), and TNF- $\alpha$  (H), in the serum of dying and recovering mice. Cytokines present in five mice per group were measured by enzyme-linked immunosorbent assay. The levels of corticosterone (E) and TNF- $\alpha$  (I) of mice were also measured after 10<sup>7</sup> PFU or 10<sup>3</sup> PFU challenges at 8 days pi. The error bars indicate the standard errors. *P* value in each graph was determined by the analysis of variance. Asterisks show the pairs that exhibit significant differences by Student *T* test in the graph that indicates *P* < 0.05 by the analysis of variance.



spleen at the time (Figs. 2C and D), indicating that direct viral infection of thymocytes and splenocytes is unlikely to be the main cause of their atrophy.

Thymic depletion and body weight loss are the main features of the systemic stress response (Dunn et al., 1989; Savino, 2006). These data therefore raise the possibility that severe systemic stress responses were elicited in dying mice. Corticosterone is a major glucocorticoid hormone, the levels of which are elevated under a stress response condition (Dunn et al., 1989; Savino, 2006). Measurement of the levels of corticosterone revealed that they were significantly increased in dying mice compared with mock-infected mice and surviving mice (Fig. 7D), indicating that dying mice exhibited a severe stress response.

However, decreased numbers of thymocytes and splenocytes (data not shown) and increased levels of corticosterone (Fig. 7E) were observed in mice early after infection with high ( $10^7$  PFU) but not low ( $10^3$  PFU) virus challenge doses. Therefore, severe systemic stress response appears to be a common factor in the lethal process of both early and late death.

#### *Increased levels of TNF- $\alpha$ in dying mice exhibiting late death*

We subsequently investigated the levels of inflammatory cytokines in the sera of infected mice at 13 days pi. The levels of IFN- $\gamma$ , RANTES and TNF- $\alpha$  were increased in both dying and recovering mice compared with mock-infected mice (Figs. 7F to H), although the levels of other inflammatory cytokines involving IL-1 $\beta$ , IL-2, IL-4, IL-6, IL-10, IL-12 and MIP-1 $\alpha$  did not significantly differ among dying, recovering and control mice (data not shown).

Although the increased levels of IFN- $\gamma$  and RANTES were similar in dying and surviving mice, TNF- $\alpha$  levels were significantly increased in mice that eventually died (Fig. 7H). This was not the case in mice early after infection with either high or low virus challenge doses (Fig. 7I). Therefore, the increased level of TNF- $\alpha$  appeared to be a specific response of late death.

## **Discussion**

It is believed that CNS pathology is a major cause of disease development and thus mortality is determined by the relative severity of CNS pathology. However, in this study of subcutaneous infections with TBEV, we have shown that fatality is determined by a complex mechanism that includes severity of CNS pathology and systemic responses that involve stress response and increased levels of TNF- $\alpha$ .

To investigate the pathogenesis of fatal infection in detail, we distinguished dying and recovering/surviving mice by their degree of weight loss. This novel approach proved to be both simple and effective. Appetite depression probably caused the early weight loss due to decreased food and water intake (data not shown). However, it is unlikely that the undernourishment was the simple cause of death, because our preliminary data showed that subcutaneous infusion using glucose solution to compensate for weight loss did not prevent TBEV-infected mice from dying.

For CNS pathology in encephalitic flavivirus infections, virus induced direct neuronal damage is considered to be a major cause of neuronal dysfunction. High virus challenge doses rapidly induced severe CNS pathology and mice almost certainly died due to the resulting acute and widespread neuronal dysfunction. On the other hand, low virus challenge doses did not cause such severe CNS infections. Rather, brain cortex or cerebellum was preferably infected either early or late following infection. In particular, specific disappearance of Purkinje cells was observed at the late period post infection when mice died. However, surviving/recovering mice also showed the disappearance of Purkinje cells. Thus, CNS pathology alone is unlikely to determine mortality following low challenge doses.

In addition to direct virus infection, recent studies indicate that immunopathological effects on CD8<sup>+</sup> T cells contribute to the severity of CNS pathology (King et al., 2007). For example, Wang et al. (2003), showed that CD8<sup>+</sup> T cells have both protective and immunopathological effects following subcutaneous infection with the Sarafend strain of WNV in a laboratory mouse model. Experiments with MVEV also indicated that CD8<sup>+</sup> T cell function is pathogenic through the perforin and Fas/FasL lysis pathways (Licon Luna et al., 2002). Moreover, the recent work of Ruzek et al. (2009), clearly showed that CD8<sup>+</sup> T cells contribute to the survival times of mice infected with TBEV. Therefore, in addition to the direct effect of viral infections, immunopathological effects are also believed to contribute to the severity of CNS pathology. However, in our results, it was not clear if CD8<sup>+</sup> T cells correlated with the stages leading to fatality, because the numbers of infiltrating CD8<sup>+</sup> T cells were not significantly different between surviving/recovering and dying mice. Therefore, CD8<sup>+</sup> T cells may function in other ways in brain parenchyma to influence the protective/immunopathological effects. Further studies are required to define the pathological effects of CD8<sup>+</sup> T cells in TBEV infections.

For the systemic response of dying mice, we showed that the levels of TNF- $\alpha$  were increased in brains and serum. TNF- $\alpha$  is a proinflammatory cytokine that is predominantly produced by activated macrophages and T lymphocytes, but a wide range of cells and tissues can also produce TNF- $\alpha$  (Bradley, 2008). Although TNF- $\alpha$  may contribute beneficially, inappropriate or excessive production can be harmful (Bradley, 2008). A recent report showed that TNF- $\alpha$  has a protective effect against WNV during the acute phase of infection (Shrestha et al., 2008). However, it is not known if the increased levels of TNF- $\alpha$  at the late phase of infection contribute beneficially or harmfully. Our preliminary data suggest that the injections of neutralizing antibody to TNF- $\alpha$  after the onset of disease did not show significant effects on disease improvement or protection from death. Thus, further study will be necessary to decide whether or not increased levels of TNF- $\alpha$  contribute to the onset of late death.

We also showed that mice exhibited thymic and splenic atrophy following TBEV infection. Similar pathological observations have been observed in other infectious diseases and one major pathway is related to the increased levels of glucocorticoid hormone such as corticosterone in the blood (Savino, 2006). In fact, we observed that the levels of corticosterone in the serum were increased in TBEV-infected mice. Glucocorticoid is induced under stress conditions and exerts immunomodulatory effects through activation of the hypothalamic–pituitary–adrenal axis (Bailey et al., 2003; Ben-Nathan and Feuerstein, 1990; Dunn et al., 1989; Savino, 2006), suggesting that TBEV infections elicit stress responses in mice, in particular dying mice which show severe stress responses compared with recovering mice. Repeated injection with corticosterone induced depression in mice (Zhao et al., 2008). However, it is uncertain if the increased stress response directly contributes to the mortality or if the response is induced as a result of the lethal process.

Dose independent mortality induced by encephalitic flaviviruses has been recognized but has been an unresolved problem since the 1940s (King et al., 2007; Lennette, 1944). Here we have demonstrated that dose independent mortality in which mortality rates approximated to 50%, may occur following a wide range of relatively low virus challenge doses. Other encephalitic flavivirus strains exhibiting dose independent mortality also show high (e.g. 100%) and low (e.g. 20 to 60%) mortality rates following different challenge doses (Licon Luna et al., 2002; Samuel and Diamond, 2006; Vince and Grcevic, 1969; Wang et al., 2006; Wang et al., 2003). In addition, the observation of longer survival times in some animals implies late death as reported herein. Thus, late death following low virus challenge doses appears to be a key feature of dose independent mortality within the encephalitic flaviviruses. However, the precise determinants of late death have not been identified in this study.

Our previous and unpublished studies showed that some TBEV strains such as Sofjin (Far-eastern subtype), IR (Siberian subtype) and Hochosterwitz (European-subtype) exhibited dose dependent mortality following peripheral infection, whereas other strains such as Oshima, KH, VL (Far-eastern subtypes) exhibited dose independent mortality (Chiba et al., 1999; Hayasaka et al., 2001a; Hayasaka et al., 2001b; Hayasaka et al., 1999). Of note, such dose dependent strains elicited early death and 100% lethality rates even after low dose infections. Sofjin strain exhibited extremely high replication in brains compared with Oshima strain (Chiba et al., 1999), suggesting that even low dose infections reached lethal levels of infection in the CNS early after infection and neuroinvasiveness directly links to this mortality. Thus, we propose that the ability of virus to replicate in the CNS determines the pattern of mortality and the dose dependent or independent mortality. However, further study is necessary to examine whether or not different strains of TBEV present different pathogenicities in the mouse model, because the patterns of mortality are different between Sofjin and other strains of far-eastern subtypes.

In human cases, TBE takes a biphasic course of acute febrile illness and neurological syndrome, whereas mice did not exhibit elevated body temperature. However, peripheral infections and viraemia were observed in infected mice before neuronal infections. Thus, mice may also present a biphasic course of illness, although it was difficult to observe the first symptoms.

It is usually believed that human cases succumb to acute and critical neuronal dysfunction following direct viral infection of the neurons, suggesting that early death, as shown in this mouse study, possibly relates to the mechanism of mortality in human cases. In addition, our results indicate that systemic responses in late phases potentially contribute to the severity and fatality of TBE in human cases. Further elucidation of the mechanism of late death in the mouse model is an important priority to enable the development of effective treatment strategies for human TBE.

## Materials and methods

### *Virus and cells*

Stock virus of TBEV Oshima strain (Takashima et al., 1997) was prepared from cell culture medium of baby hamster kidney (BHK) cells that was infected with a previously prepared virus stock in suckling mice brains (Hayasaka et al., 2001b). The BHK cells were maintained in Eagle's Minimal Essential Medium (EMEM; Nissui Pharmaceutical Co.) containing 8% fetal calf serum (FCS). All experiments using live TBEV were performed in a biosafety level 3 laboratory of the Tokyo Metropolitan Institute for Neuroscience according to the standard BSL3 guidelines.

### *Mice*

Five-week old female C57BL/6j mice (Japan SLC Co.) were subcutaneously inoculated with a range of  $10^{-1}$ – $10^{7.8}$  PFU of TBEV diluted in EMEM containing 2% FCS. Mock-infected mice were inoculated with EMEM from the supernatant medium of BHK cells. Mice were weighed daily and observed for clinical disease symptoms including behavioral symptoms and signs of paralysis. Body temperatures of mice and the consumption of food and water were also measured daily. Morbidity was determined by the relative degree of weight loss compared with day 0. Thirteen days post infection (pi), dying and recovering mice were distinguished by the degree of weight ratio, namely mice exhibiting more than 25% or less than 25% weight loss were recognized as dying or recovering mice, respectively. The experimental protocols were approved by the Animal Care and Use Committee of the Tokyo Metropolitan Institute for Neuroscience.

### *Virus titration in tissues*

Every 2 days, three to five mice were sacrificed and blood, lung, thymus, spleen, brain and spinal cord were collected following perfusion with cold phosphate-buffered saline (PBS). Brains were also collected and dissected to provide four separate fractions, i.e. the brain cortex, thalamus, cerebellum and brainstem. Until they were used, these organs were stored at  $-80^{\circ}\text{C}$ . Each organ was homogenized in ten volumes of PBS containing 10% FCS and diluted with EMEM with 2% FCS. Virus titers were determined by plaque forming assays (Shirato et al., 2004) using BHK cells and were expressed as PFU/g tissue.

### *Histopathological examination*

Mice inoculated with TBEV were anesthetized and perfused with 10% phosphate-buffered formalin. Fixed tissues of thymus, lung, liver, kidney, spleen, small intestine, brain, spinal cord, and maxilla including nasal cavity were routinely embedded in paraffin, sectioned, and stained with hematoxylin and eosin. Immunohistochemical detection of the TBEV antigens was performed as described previously (Nagata et al., 2007). Rabbit polyclonal antibody against E protein was used to detect TBEV antigens (Yoshii et al., 2004).

### *Recovery of leukocytes from brain, thymus and spleens*

Recovery of leukocytes was performed using previously described methods (Hayasaka, Ennis, and Terajima, 2007; Shrestha and Diamond, 2004). Briefly, brain leukocytes were isolated from mice infected with mock,  $10^7$  or  $10^3$  PFU of virus at 8 and 13 days pi. After perfusion with cold PBS, brains were removed and placed on ice in RPMI containing 5% FCS (Nissui Pharmaceutical Co.). Brains were strained and homogenized gently with a 70  $\mu\text{m}$  cell strainer (BD Biosciences). After washing with RPMI, the cell suspension was layered onto a 70% and 30% Percoll gradient (GE Healthcare Bio-Sciences AB) and centrifuged at  $800\times g$  for 45 min at  $23^{\circ}\text{C}$ . The leukocytes were collected from between the 70% and 30% interface. Thymocytes and splenocytes were also recovered from these mice. Cells were strained with a 70  $\mu\text{m}$  cell strainer (BD Biosciences) and lysed with RBC lysis buffer (Sigma-Aldrich). After washing, cells were resuspended in RPMI medium. Isolated cells were counted and kept on ice until the staining procedure.

### *Flow cytometric analysis of cell-surface antigens*

Brain leukocytes, thymocytes and splenocytes were washed and blocked with Rat Anti-Mouse CD16/32 (Fc Receptor) (Beckman Coulter) in FACS buffer (PBS containing 0.1% BSA and 0.1% sodium azide). Cells were stained with a mixture of different fluorescent-labeled antibodies directed at surface phenotypic markers, CD45, CD3 $\epsilon$ , CD4, CD8 $\alpha$ , CD19, NK1.1 (Ly-55), Ly-6G (GR-1) (Beckman Coulter) and F4/80 (AbD Serotec) and then fixed with 4% paraformaldehyde overnight. The stained cells were analyzed by Epics Altra (Beckman Coulter). Leukocytes were recognized by characteristic size (forward scatter, FSC), granularity (side scatter, SSC) and CD45 expression. CD8 $^{+}$  T cells and B cells were recognized by CD3 and CD8 expression, and CD19 expression in CD45 $^{+}$  leukocytes, respectively. Thymocytes and splenocytes were recognized by their characteristic size. CD4 $^{+}$ CD8 $^{+}$  double positive cells were recognized by the expression of CD4 $^{+}$  and CD8 $^{+}$  in the thymocytes.

### *Quantitative estimation of the expression of inflammatory cytokines in brains*

Five mice in each group were infected with mock,  $10^7$  or  $10^3$  PFU of virus and brains were collected after perfusion with cold PBS at 8 and

13 days pi. Freshly isolated brains were immediately immersed in RNAlater (Ambion). Total RNA was extracted using RNeasy Lipid Tissue Mini Kit (Qiagen) according to the manufacturer's instruction. The expression levels of cytokines were measured by real time-PCR as demonstrated previously (Fuji et al., 2008). The copy numbers were calculated as a ratio of the copy numbers of internal control glyceraldehyde-3-phosphate dehydrogenate (GAPDH).

#### Estimations of hormones and cytokine levels in the serum

Serum samples were collected from five mice infected with mock,  $10^7$  or  $10^3$  PFU of virus at 8 and 13 days pi. The levels in the serum were measured using competitive enzyme immunoassay and sandwich enzyme-linked immunosorbent assay kits for corticosterone (Assay-Pro), IFN- $\gamma$ , TNF- $\alpha$ , IL-1 $\beta$ , IL-2, IL-4, IL-6, IL-10, IL-12 (Endogen), MIP-1 $\alpha$ , RANTES (R&D Systems) according to the manufacturer's instructions.

#### Statistical analyses

The analysis of variance and Student *T* test were used for statistical analysis to assess the significant differences of the degree of weight change, viral loads, the numbers of leukocytes, the expression levels of cytokines in brains and serum. *P* value < 0.05 was considered statistically significant.

#### Acknowledgments

We thank Kentarou Yoshii of the Graduate School of Veterinary Medicine, Hokkaido University, Ayako Harashima of the Department of Pathology, National Institute of Infectious Diseases for the experiments of histopathology, Kazutaka Kitaura of the Clinical Research Center, National Sagami Hospital, and Yuko Abe, Yasuko Yamashita, Seiya Yamayoshi and Mami Tanaka of Tokyo Metropolitan Institute for Neuroscience.

This work was supported by KAKENHI [Grant-in-Aid for Young Scientists (B) (19780230)] from the Ministry of Education, Culture, Sports, Science, and Technology, Japan, and Health Grants for Research on Emerging and Re-emerging Infectious Diseases from the Ministry of Health, Labour and Welfare, Japan. EAG is supported by the EU sixth Framework Structural Genomics Project, Vizier (Contract: LSHG-CT-2004-511960).

#### References

Albrecht, P., 1968. Pathogenesis of neurotropic arbovirus infections. *Curr. Top Microbiol. Immunol.* 43, 44–91.

Bailey, M., Engler, H., Hunziker, J., Sheridan, J.F., 2003. The hypothalamic–pituitary–adrenal axis and viral infection. *Viral Immunol.* 16 (2), 141–157.

Ben-Nathan, D., Feuerstein, G., 1990. The influence of cold or isolation stress on resistance of mice to West Nile virus encephalitis. *Experientia* 46 (3), 285–290.

Bradley, J.R., 2008. TNF-mediated inflammatory disease. *J. Pathol.* 214 (2), 149–160.

Burke, S.D., Monath, P.T., 2001. Flaviviruses. In: Knipe, D.M., Howley, P.M., Griffin, D.E., Lamb, R.A., Martin, M.A., Roizman, B., Straus, S.E. (Eds.), *Fields Virology*. Lippincott Williams & Wilkins, Philadelphia, PA, pp. 991–1041.

Byrne, S.N., Halliday, G.M., Johnston, L.J., King, N.J., 2001. Interleukin-1beta but not tumor necrosis factor is involved in West Nile virus-induced Langerhans cell migration from the skin in C57BL/6 mice. *J. Invest. Dermatol.* 117 (3), 702–709.

Charrel, R.N., Attoui, H., Butenko, A.M., Clegg, J.C., Deubel, V., Frolova, T.V., Gould, E.A., Gritsun, T.S., Heinz, F.X., Labuda, M., Lashkevich, V.A., Loktev, V., Lundkvist, A., Lvov, D.V., Mandl, C.W., Niedrig, M., Papa, A., Petrov, V.S., Plyusnin, A., Randolph, S., Suss, J., Zlobin, V.I., de Lamballerie, X., 2004. Tick-borne virus diseases of human interest in Europe. *Clin. Microbiol. Infect.* 10 (12), 1040–1055.

Chiba, N., Iwasaki, T., Mizutani, T., Kariwa, H., Kurata, T., Takashima, I., 1999. Pathogenicity of Tick-borne encephalitis virus isolated in Hokkaido, Japan in mouse model. *Vaccine* 17 (7–8), 779–787.

Couderc, T., Guivel-Benhassine, F., Calao, V., Gosselin, A.S., Blondel, B., 2002. An ex vivo murine model to study poliovirus-induced apoptosis in nerve cells. *J. Gen. Virol.* 83 (Pt. 8), 1925–1930.

Dumpis, U., Crook, D., Oksi, J., 1999. Tick-borne encephalitis. *Clin. Infect. Dis.* 28 (4), 882–890.

Dunn, A.J., Powell, M.L., Meitin, C., Small Jr., P.A., 1989. Virus infection as a stressor:

influenza virus elevates plasma concentrations of corticosterone, and brain concentrations of MHPG and tryptophan. *Physiol. Behav.* 45 (3), 591–594.

Ecker, M., Allison, S.L., Meixner, T., Heinz, F.X., 1999. Sequence analysis and genetic classification of Tick-borne encephalitis viruses from Europe and Asia. *J. Gen. Virol.* 80 (Pt. 1), 179–185.

Fujii, Y., Kitaura, K., Nakamichi, K., Takasaki, T., Suzuki, R., Kurane, I., 2008. Accumulation of T-cells with selected T-cell receptors in the brains of Japanese encephalitis virus-infected mice. *Jpn. J. Infect. Dis.* 61 (1), 40–48.

Garcia-Tapia, D., Hasset, D.E., Mitchell Jr., W.J., Johnson, G.C., Kleiboeker, S.B., 2007. West Nile virus encephalitis: sequential histopathological and immunological events in a murine model of infection. *J. Neurovirol.* 13 (2), 130–138.

Gelpi, E., Preusser, M., Garzuly, F., Holzmann, H., Heinz, F.X., Budka, H., 2005. Visualization of Central European Tick-borne encephalitis infection in fatal human cases. *J. Neuropathol. Exp. Neurol.* 64 (6), 506–512.

Gelpi, E., Preusser, M., Laggner, U., Garzuly, F., Holzmann, H., Heinz, F.X., Budka, H., 2006. Inflammatory response in human Tick-borne encephalitis: analysis of postmortem brain tissue. *J. Neurovirol.* 12 (4), 322–327.

Hayasaka, D., Ennis, F.A., Terajima, M., 2007. Pathogenesis of respiratory infections with virulent and attenuated vaccinia viruses. *Virology* 361 (1), 4–22.

Hayasaka, D., Goto, A., Yoshii, K., Mizutani, T., Kariwa, H., Takashima, I., 2001a. Evaluation of European Tick-borne encephalitis virus vaccine against recent Siberian and far-eastern subtype strains. *Vaccine* 19 (32), 4774–4779.

Hayasaka, D., Ivanov, L., Leonova, G.N., Goto, A., Yoshii, K., Mizutani, T., Kariwa, H., Takashima, I., 2001b. Distribution and characterization of Tick-borne encephalitis viruses from Siberia and far-eastern Asia. *J. Gen. Virol.* 82 (Pt. 6), 1319–1328.

Hayasaka, D., Gritsun, T.S., Yoshii, K., Ueki, T., Goto, A., Mizutani, T., Kariwa, H., Iwasaki, T., Gould, E.A., Takashima, I., 2004. Amino acid changes responsible for attenuation of virus neurovirulence in an infectious cDNA clone of the Oshima strain of Tick-borne encephalitis virus. *J. Gen. Virol.* 85 (Pt. 4), 1007–1018.

Hayasaka, D., Suzuki, Y., Kariwa, H., Ivanov, L., Volkov, V., Demenev, V., Mizutani, T., Gojobori, T., Takashima, I., 1999. Phylogenetic and virulence analysis of Tick-borne encephalitis viruses from Japan and far-Eastern Russia. *J. Gen. Virol.* 80 (Pt. 12), 3127–3135.

Holzmann, H., 2003. Diagnosis of Tick-borne encephalitis. *Vaccine* 21 (Suppl. 1), S36–S40.

Iwasaki, Y., Zhao, J.X., Yamamoto, T., Konno, H., 1986. Immunohistochemical demonstration of viral antigens in Japanese encephalitis. *Acta Neuropathol.* 70 (1), 79–81.

King, N.J., Getts, D.R., Getts, M.T., Rana, S., Shrestha, B., Kesson, A.M., 2007. Immunopathology of flavivirus infections. *Immunol. Cell. Biol.* 85 (1), 33–42.

Lenette, E.H., 1944. Influence of age on the susceptibility of mice to infection with certain neurotropic viruses. *J. Immunol.* 49, 175–191.

Liao, Y., Tang, Z.Y., Liu, K.D., Ye, S.L., Huang, Z., 1997. Apoptosis of human BEL-7402 hepatocellular carcinoma cells released by antisense H-ras DNA—in vitro and in vivo studies. *J. Cancer Res. Clin. Oncol.* 123 (1), 25–33.

Licon Luna, R.M., Lee, E., Mullbacher, A., Blanden, R.V., Langman, R., Lobigs, M., 2002. Lack of both Fas ligand and perforin protects from flavivirus-mediated encephalitis in mice. *J. Virol.* 76 (7), 3202–3211.

Lindquist, L., Vapalahti, O., 2008. Tick-borne encephalitis. *Lancet* 371 (9627), 1861–1871.

Mandl, C.W., 2005. Steps of the Tick-borne encephalitis virus replication cycle that affect neuropathogenesis. *Virus Res.* 111 (2), 161–174.

Monath, T.P., 1986. Pathology of the flaviviruses. In: Schlesinger, S., Schlesinger, M.J. (Eds.), *The Togaviridae and Flaviviridae*. Plenum Press, New York, pp. 375–440.

Monath, T.P., Cropp, C.B., Bowen, G.S., Kemp, G.E., Mitchell, C.J., Gardner, J.J., 1980. Variation in virulence for mice and rhesus monkeys among St. Louis encephalitis virus strains of different origin. *Am. J. Trop. Med. Hyg.* 29 (5), 948–962.

Nagata, N., Iwata, N., Hasegawa, H., Fukushi, S., Yokoyama, M., Harashima, A., Sato, Y., Saijo, M., Morikawa, S., Sata, T., 2007. Participation of both host and virus factors in induction of severe acute respiratory syndrome (SARS) in F344 rats infected with SARS coronavirus. *J. Virol.* 81 (4), 1848–1857.

Pogodina, V.V., Savinov, A.P., 1964. Variation in the pathogenicity of viruses of the Tick-borne encephalitis complex for different animal species. I. Experimental infection of mice and hamsters. *Acta. Virol.* 8, 424–434.

Prikhod ko, G.G., Prikhod ko, E.A., Cohen, J.I., Pletnev, A.G., 2001. Infection with *Langat flavivirus* or expression of the envelope protein induces apoptotic cell death. *Virology* 286 (2), 328–335.

Robertson, S.J., Mitzel, D.N., Taylor, R.T., Best, S.M., Bloom, M.E., 2009. Tick-borne flaviviruses: dissecting host immune responses and virus countermeasures. *Immunol. Res.* 43 (1–3), 172–186.

Ruzek, D., Salat, J., Palus, M., Gritsun, T.S., Gould, E.A., Dykova, I., Skalova, A., Jelinek, J., Kopecky, J., Grubhoffer, L., 2009. CD8+ T-cells mediate immunopathology in Tick-borne encephalitis. *Virology* 384 (1), 1–6.

Samuel, M.A., Diamond, M.S., 2006. Pathogenesis of West Nile virus infection: a balance between virulence, innate and adaptive immunity, and viral evasion. *J. Virol.* 80 (19), 9349–9360.

Savino, W., 2006. The thymus is a common target organ in infectious diseases. *PLoS Pathog.* 2 (6), e62.

Shirato, K., Miyoshi, H., Goto, A., Ako, Y., Ueki, T., Kariwa, H., Takashima, I., 2004. Viral envelope protein glycosylation is a molecular determinant of the neuroinvasiveness of the New York strain of West Nile virus. *J. Gen. Virol.* 85 (Pt. 12), 3637–3645.

Shrestha, B., Diamond, M.S., 2004. Role of CD8+ T cells in control of West Nile virus infection. *J. Virol.* 78 (15), 8312–8321.

Shrestha, B., Gottlieb, D., Diamond, M.S., 2003. Infection and injury of neurons by West Nile encephalitis virus. *J. Virol.* 77 (24), 13203–13213.

Shrestha, B., Zhang, B., Purtha, W.E., Klein, R.S., Diamond, M.S., 2008. Tumor necrosis factor alpha protects against lethal West Nile virus infection by promoting trafficking of mononuclear leukocytes into the central nervous system. *J. Virol.* 82 (18), 8956–8964.



- Sokol, F., Libikova, H., Zemla, J., 1959. Infectious ribonucleic acid from mouse brains infected with Tick-borne encephalitis virus. *Nature* 184 (Suppl. 20), 1581.
- Takashima, I., Morita, K., Chiba, M., Hayasaka, D., Sato, T., Takezawa, C., Igarashi, A., Kariwa, H., Yoshimatsu, K., Arikawa, J., Hashimoto, N., 1997. A case of Tick-borne encephalitis in Japan and isolation of the virus. *J. Clin. Microbiol.* 35 (8), 1943–1947.
- Vince, V., Grcevic, N., 1969. Development of morphological changes in experimental Tick-borne meningoencephalitis induced in white mice by different virus doses. *J. Neurol. Sci.* 9 (1), 109–130.
- Wang, Y., Lobigs, M., Lee, E., Koskinen, A., Mullbacher, A., 2006. CD8(+) T cell-mediated immune responses in West Nile virus (Sarafend strain) encephalitis are independent of gamma interferon. *J. Gen. Virol.* 87 (Pt. 12), 3599–3609.
- Wang, Y., Lobigs, M., Lee, E., Mullbacher, A., 2003. CD8<sup>+</sup> T cells mediate recovery and immunopathology in West Nile virus encephalitis. *J. Virol.* 77 (24), 13323–13334.
- Yoshii, K., Konno, A., Goto, A., Nio, J., Obara, M., Ueki, T., Hayasaka, D., Mizutani, T., Kariwa, H., Takashima, I., 2004. Single point mutation in Tick-borne encephalitis virus prM protein induces a reduction of virus particle secretion. *J. Gen. Virol.* 85 (Pt. 10), 3049–3058.
- Zhao, Y., Ma, R., Shen, J., Su, H., Xing, D., Du, L., 2008. A mouse model of depression induced by repeated corticosterone injections. *Eur. J. Pharmacol.* 581 (1–2), 113–120.